BIOCHEMISTRY
including biophysical chemistry & molecular biology

Article

pubs.acs.org/biochemistry

Redirecting P450 EryK Specificity by Rational Site-Directed Mutagenesis

Linda Celeste Montemiglio,[†] Alberto Macone,[†] Chiara Ardiccioni,[‡] Giovanna Avella,[†] Beatrice Vallone,*[,†,§] and Carmelinda Savino*[,†,§]

[†]Istituto Pasteur-Fondazione Cenci Bolognetti and Istituto di Biologia e Patologia Molecolari del CNR, Dipartimento di Scienze Biochimiche "A. Rossi Fanelli", Sapienza Università di Roma, Piazzale A. Moro 5, 00185 Rome, Italy

[‡]Departments of Physiology & Cellular Biophysics, Columbia University College of Physicians & Surgeons, Russ Berrie Pavilion, 1150 St. Nicholas Avenue, New York, New York 10032, United States

Supporting Information

ABSTRACT: The C-12 hydroxylase EryK is a bacterial cytochrome P450, active during one of the final tailoring steps of erythromycin A (ErA) biosynthesis. Its tight substrate specificity, restricted to the metabolic intermediate ErD, leads to the accumulation in the culture broth of a shunt metabolite, ErB, that originates from the competitive action of a methyltranferase on the substrate of EryK. Although the methylation of the mycarosyl moiety represents the only difference between the two metabolites, EryK exhibits very low conversion of ErB in ErA via a parallel pathway. Given its limited antimicrobial activity and its moderate toxicity, contamination by such a byproduct decreases the yield and purity of the antibiotic. In this study, EryK has been redesigned to make it suitable for industrial application. Taking advantage of the three-dimensional structure of the enzyme in complex with ErD, three single active-site mutants of EryK (M86A, H88E, and E89L) have been designed to allow hydroxylation of the nonphysiological substrate ErB. The binding and catalytic properties of these three variants on both ErD and ErB have been analyzed. Interestingly, we found the mutation of Met 86 to Ala to yield enzymatic activity on both ErB and ErD. The three-dimensional structure of the complex of mutated EryK with ErB revealed that the mutation allows ErB to accommodate in the active site of the enzyme and to induce its closure, thus assuring the progress of the catalytic reaction. Therefore, by single mutation the fine substrate recognition, active site closure, and locking were recovered.

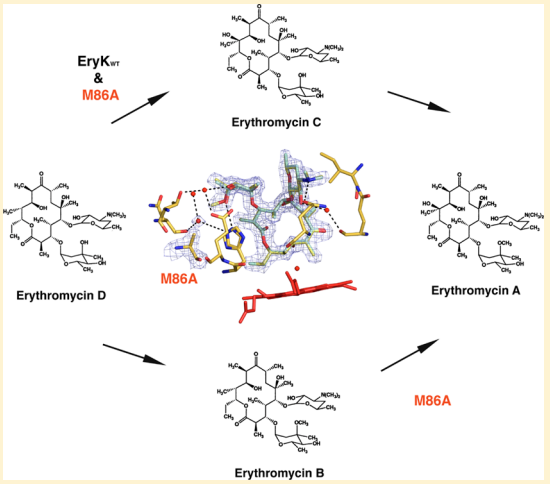

Erythromycin A (ErA) is one of the most studied and characterized microbial metabolites, well known for its antibiotic properties. Introduced into clinical practice over 50 years ago, it is still widely used in the treatment of infectious diseases caused by gram-positive bacteria.[1−5] During the last two decades, much of the interest in ErA has been devoted to its potential use as a substrate for further chemical modifications in order to yield novel macrolide analogues with improved biological activities.[6] Several ErA-based semisynthetic derivatives, such as azithromycin and clarithromycin, are now commercially available and show broader spectra of efficacy and improved pharmacokinetic profiles.[7−12] The large clinical use of this antibiotic and the expanded diffusion of its derivatives demand the continuous and massive production of ErA. Given the complexity of its structure, the total chemical synthesis of the molecule[13] is unsuitable for large-scale production. ErA is commonly produced at the industrial level by fermentation, using overproducing strains of *Saccharomyces erythraeus*.[14] However, the yield and purity of the final antibiotic product are affected by the accumulation in the culture broth of erythromycin intermediates (Ers) that occurs during the ErA biosynthetic pathway. Such compounds are generally removed during the postfermentation stage since they are biologically less active and cause greater side effects.[15] The imperative need to reduce the amount of such impurities, limited within 5% by the European Pharmacopoeia criteria,[16] complicates the downstream process of purification and increases production costs.

The critical step for Ers accumulation is the conversion of erythromycin D (ErD) to erythromycin C (ErC) that occurs during the late phase of ErA biosynthesis (Figure 1). The reaction is catalyzed by a cytochrome P450, EryK (CYP113A1),[3,11,17] that acts as a hydroxylase on the C12 of the macrolactone ring of ErD. The released product, ErC, undergoes O-methylation of the mycarose sugar moiety by the methyltransferase EryG to give ErA (Figure 1). Nevertheless,

Received: February 21, 2013
Revised: April 18, 2013
Published: April 19, 2013

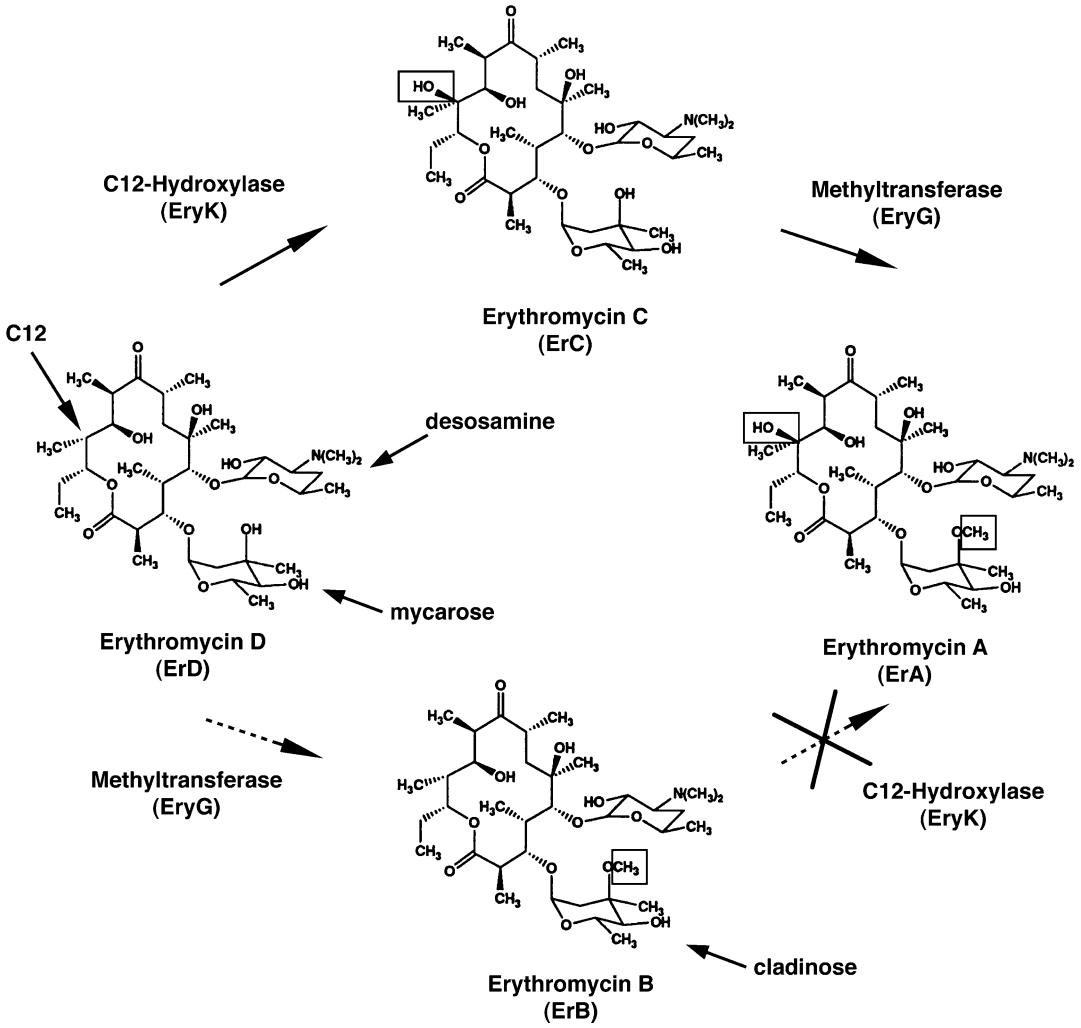

Figure 1. Schematic representation of the final steps of ErA biosynthesis. The ErA biosynthetic pathway consists of a first constructive phase in which the macrocyclic lactone is formed and a second phase in which several tailoring enzymes introduce specific functional groups on the ring. The C-12 hydroxylase EryK is active during the final steps of the second phase reported here; its substrate, ErD, if hydroxylated (ErC), undergoes an O-methylation to give ErA; if ErD is methylated (ErB), then it cannot be recognized by EryK, becoming a shunt metabolite and decreasing the drug production yield. The chemical structures of ErD, ErB, ErC, and ErA are shown. C-12, desosamine, mycarose, and cladinose are labeled. The hydroxyl group inserted by EryK on the C-12 of the macrolactone ring and the methyl group on the C3′-OH of cladinose are highlighted with black squares. The dashed arrows indicate the shunt pathway.

EryG may also competitively act on ErD, thus generating a parallel pathway that results in the production of a shunt metabolite, erythromycin B (ErB). Sugar methylation, which represents the only difference between ErD and ErB (Figure 1), is sufficient to prevent the binding of ErB to EryK, giving rise to significant shunt product accumulation.[18]

Previous work based on metabolic engineering described the improvement obtained by genetically modulating the amount of EryK and EryG genes in *S. eryhtraeus*, thus increasing the titer by almost 25% and improving the purity of ErA, even on an industrial scale.[19,20] Nevertheless, these strains suffer from genetic instability, partially overcome by introducing an artificial *attB* cassette in the chromosome of the industrial *S. erythraeus* strain, HL3168 E3, thus avoiding unpredictable nonspecific recombination.[21]

The recent availability of the three-dimensional structure of EryK in complex with its substrate ErD (ErD−EryK[22]) offers the possibility to redesign the enzyme allowing it to hydroxylate the unnatural substrate ErB, while maintaining its enzymatic activity against ErD. Previous experimental studies performed *in vitro*, in which the EryK preference for ErD had been proved to be about 1200−1900-fold over that of ErB, identified the mycarosyl unit as a critical feature of productive substrate binding.[18] This consideration has been confirmed by analyzing the structure of the ErD−EryK complex, whereby the key contacts that allow discrimination against the undesired shunt metabolite were identified. It was observed that a methyl group on the 3′-OH of the mycarosyl moiety, as in ErB, would collide with three amino acids on the BC loop (Met 86, His 88, and Glu 89), thus hindering the complete closure of the enzyme on the substrate, its locking, and the progress of the catalytic reaction.[22]

In the present work, three site-specific mutants of the identified residues were designed with the aim of producing a promiscuous form of EryK able to bind and to hydroxylate both ErD and the metabolic shunt intermediate, ErB. Met 86, His 88, and Glu 89 were mutated to allow accommodation of the bulky methoxyl group of the cladinose of ErB in the same region of the active site that normally accepts the hydroxyl function of mycarose. We report and briefly discuss binding and

dx.doi.org/10.1021/bi400223j | *Biochemistry* 2013, 52, 3678−3687

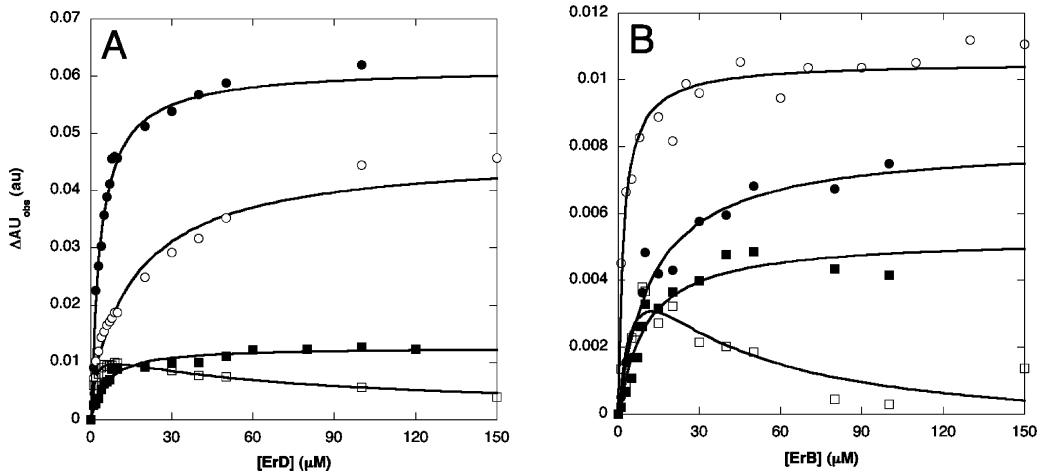

Figure 2. Equilibrium binding titrations of $EryK_{WT}$ and mutants with ErD and ErB. The measured absorbance delta values (where $\Delta AU_{obs} = A_{390\ nm} - A_{420\ nm}$) as a function of ErD (panel A) and ErB (panel B) concentration are shown for $EryK_{WT}$ (filled circles) and mutants M86A, H88E, and E89L (open circles, filled squares, and open squares, respectively). In each experiment, absorbance was monitored at 420 and 390 nm using 2 μM enzyme at 298 K in 50 mM Tris·HCl at pH 7.5. Data were fitted to eq 1 (fits are shown as solid lines) to determine the dissociation constants, K_D (Table 1). ErD−$EryK_{WT}$ binding data refer to ref 22.

catalytic properties of the three EryK variants on both ErD and ErB. Depending on the mutation, binding and enzymatic activity on ErD are differently affected. By analyzing the EryK mutant behavior toward ErB, we identified the mutation on Met 86 as the sole form of EryK that is able to bind and hydroxylate the shunt compound ErB, as well as ErD. Analysis of the crystal structure of the Met 86 mutant bound to ErB reveals that the shunt product adopts the same position and orientation as those of ErD in the active site of wild type EryK[22] and induces the enzyme locking required for the progress of the enzymatic reaction.

MATERIALS AND METHODS

Site-Directed Mutagenesis, Expression, and Purification. M86A, H88E, and E89L EryK mutants were produced by using the QuickChange kit (Stratagene, La Jolla, CA) according to the manufacturer's instructions and using the pET28b(+)-EryK construct (kindly supplied by Biotica Technology Ltd., U.K.) as a template. Single mutations were introduced by overlap extension PCR by using the following mismatching oligonucleotides as primers (altered codons are in boldface): M86A, ccgacgccgggc**gcg**atccacgagat; H88E, ccgggcatgatc**cac**gagatcgacccg; and E89L, cgcatgatccac**ctg**atcgacccgccg. In order to confirm the presence of the desired mutation, each plasmid was sequenced. All mutants were expressed in *E. coli* BL21 (DE3) (Invitrogen, Carlsbad, CA, USA) and purified as previously described for wild type EryK.[23] Preliminary optical characterization revealed that all mutants show a Soret band maximum at 420 nm, the same as that of the wild type, with the exception of the H88E mutant that displays a slight red shift of the maximum at 422 nm (data not shown).

Equilibrium Binding Analyses. All mutants were tested for binding to both the metabolic intermediates, ErD and ErB (Figure 1). ErD (kindly supplied by Biotica Technology Ltd., U.K.) and ErB (European Pharmacopoeia Reference Standard) stock solutions (14 and 20 mM, respectively) were prepared in deionized water and dimethyl sulfoxide (DMSO), respectively. The enzymes (2 μM) were titrated at 298 K with ErD and ErB in a total volume of 800 μL of 50 mM Tris·HCl buffer at pH 7.5. The final substrate concentration covered a range from 0 to 150 μM for both ErD and ErB, thus keeping DMSO below 1% to avoid interference with the optical spectra.[18]

UV visible spectra (200−820 nm) were recorded after each substrate addition, and the appropriate blank was subtracted. The measured absorbance delta values (where $\Delta AU_{obs} = A_{390\ nm} - A_{420\ nm}$) were plotted against substrate concentration (Figure 2A,B).

The dissociation constant (K_D) was estimated using the Kaleidagraph software package. A nonlinear regression analysis was applied using a hyperbolic equation as follows:

$$\Delta AU_{obs} = \Delta AU_{max}[S]/(K_D + [S]) \quad (1)$$

where ΔAU_{obs} is the absorbance difference, ΔAU_{max} is the maximum absorbance difference extrapolated to infinite ligand concentration, and [S] is the substrate analytical concentration. Data were globally fitted with the program Prism (Graphpad).

Spectrophotometric Assay for Enzymatic Activity. The hydroxylase activity of EryK wild type ($EryK_{WT}$) and mutants was tested with respect to both the physiological substrate ErD and the secondary metabolite ErB. The enzymatic assay was carried out using as electron donor the system ferredoxin/ferredoxin NADP+ reductase that uses the cofactor NADPH ($\varepsilon_{340\ nm}$= 6220 M^{-1} cm^{-1}) as the source of electrons.[18]

In a total volume of 50 μL, 1 μM enzyme, 9 μM spinach ferredoxin (Sigma Aldrich), 2.5 μM spinach ferredoxin NADP+ reductase (Sigma Aldrich), 50 mM Tris·HCl at pH 7.5, and substrate (from 0 to a maximum of 800 μM) were mixed together in a 1 cm light path cuvette mounted on a constant temperature cell holder equilibrated at 303 K. NADPH (Sigma Aldrich) at a final concentration of 200 μM was added to start the reaction. Assuming a 1:1 stoichiometry between NADPH consumption and substrate hydroxylation, initial velocities were measured spectroscopically at different substrate concentrations by monitoring the rate of absorbance decay at 340 nm over time using a Jasco J650 spectrophotometer in kinetic mode, setting 200 s as run time. Initial rates were determined by applying a linear fit to the linear region of the time trace, determined to be the first 30 s. Initial velocity data were fitted using the Kaleidagraph software package by following the hyperbolic equation of Michaelis−Menten:

dx.doi.org/10.1021/bi400223j | *Biochemistry* 2013, 52, 3678−3687

$$\nu = \frac{V_{max}[S]}{K_M + [S]} \quad (2)$$

where ν is the initial velocity of the reaction, V_{max} is the maximum velocity of the reaction corresponding to substrate saturation of the enzyme, K_M is the Michaelis−Menten constant, and [S] is the substrate analytical concentration.

GC/MS Analyses of the Hydroxylation Product. In order to analyze the hydroxylation product of the $EryK_{WT}$ and M86A mutants using ErB as a substrate, 1 μM of both enzymes has been incubated in independent experiments with 70 μg of ErB in the presence of 20 μM spinach ferredoxin, 0.2 units of spinach NADP+ reductase, 1 mM NADP+, 7.5 mM glucose-6-phosphate, and 0.8 units of glucose-6-phosphate dehydrogenase in a final volume of 620 μL of 50 mM Tris·HCl, at pH 7.5, for 60 min at 303 K.[18]

Two hundred microliter aliquots of each sample were extracted, dried under a stream of nitrogen, resuspended in 20 μL of methanol, and directly injected in GC-MS (1 μL). GC-MS analyses were performed on an Agilent 6850A gas chromatograph coupled to a 5973N quadrupole mass selective detector (Agilent Technologies, Palo Alto, CA, USA). Chromatographic separations were carried out on an Agilent HP5 ms fused-silica capillary column (30 m × 0.25 mm i.d.) coated with 5%-phenyl-95%-dimethylpolysiloxane (film thickness 0.25 μm) as the stationary phase. The injection mode was splitless at a temperature of 553 K. The column temperature program was 373 K (1 min), then changed to 573 K at a rate of 298 K/min, and held for 5 min. The carrier gas was helium at a constant flow of 1.0 mL/min. The ionizing energy was 70 eV (ion source 553 K; ion source vacuum 10^{-5} Torr). Mass spectra were collected both in the full-scan mode within the m/z scan range of 50−700 amu, and in the selected ion monitoring (SIM) mode checking the ion m/z 158, the most abundant in both ErA and ErB fragmentation pattern.[24] Components of the assay mixtures were identified by comparison to retention times and mass spectra of authentic standards: ErB (European Pharmacopoeia Reference Standard) and ErA (Sigma Aldrich, St.Louis, MO, USA).

Furthermore, the efficiency of the M86A mutant in NADPH consumption for product formation with respect to the $EryK_{WT}$ has been tested. In a total volume of 750 μL, 1 μM M86A mutant, 9 μM spinach ferredoxin, 170 μM NADPH, 50 mM Tris·HCl, at pH 7.5, and 40 μg of both ErD and ErB in independent experiments were mixed together in a 1 cm light path cuvette mounted in a constant temperature cell holder equilibrated at 303 K. After the addition of 2.5 μM spinach NADP+ reductase, the reactions were run at 303 K. NADPH consumption has been spectroscopically followed by monitoring the rate of absorbance decay at 340 nm over time using a Jasco J650 spectrophotometer in kinetic mode. The same procedure has been also followed to test the NADPH consumption efficiency of $EryK_{WT}$ for ErD conversion. The reactions were halted by adding 100 μL of methanol when the 50% of the initial NADPH has been consumed. Then, a 200 μL aliquot of each sample was extracted, dried under a stream of nitrogen, resuspended in 20 μL of methanol, and directly injected into the GC-MS (1 μL). GC-MS analyses were performed on an Agilent 6850A gas chromatograph coupled to a 5973N quadrupole mass selective detector (see above for experimental details). In order to obtain a reliable estimation of the amount of substrate consumed, the intensity of the peaks corresponding to ErD or ErB at the end of the reaction has been compared to the intensity of the relative peaks observed injecting the initial amount of ErD or ErB for each single experiment. Components of the assay mixtures were identified by comparison to retention times and mass spectra of authentic standards.

X-ray Crystallography. Crystals of M86A in complex with ErB (ErB−M86A) were prepared by using the protein at a concentration of 19 mg/mL in 10 mM Tris·HCl at pH 8.0. Crystallization screening was carried out at 294 K using the hanging-drop vapor diffusion method.[25] Best crystals were obtained in 25% PEG 3350, 0.1 M Tris·HCl, at pH 8.5, and 0.2 M CH_3COONH_4.

Diffraction data of crystals of the ErB−M86A complex were collected at 100 K at ID23.2 microfocus beamline using a MAR CCD detector at the ESRF (Grenoble, France). Data were indexed, integrated, and scaled by using the HKL2000 suite,[26] and the CCP4 program suite (Collaborative Computational Project No.4, 1994[27]) was used for subsequent structure refinement.

Crystals of ErB−M86A were isomorphous with those of $EryK_{WT}$ in complex with the substrate ErD (PDB code 2JJO[22]); therefore, the atomic coordinates of this model were used to determine the ErB−M86A structure by the Fourier difference method.

Refinement was carried out with Refmac5 in CCP4,[28] followed by model building and manual adjustment performed by COOT.[29,30] Ramachandran statistics indicate that only one amino acid, Ile 392, is close to the forbidden region as in the structure of ErD−EryK complex.[22] The first 20 N-terminal residues are missing in the model due to insufficient electron density. Final crystallographic statistics are shown in Table 2. All figures were produced with PyMOL (http://pymol.sourceforge.net). The atomic coordinates and structure factors have been deposited in the RCSB Protein Data Bank (PDB code 3ZKP).

RESULTS

Design of EryK Mutants. It has been known since 1995 that EryK cannot catalyze C12 hydroxylation with ErB as a substrate.[18] By inspection of the structure of wild type EryK in complex with the physiological substrate, the structural element that appears as the determinant for ErD selection is the mycarosyl moiety on C3 of the macrolactone ring. Mycarose is mainly involved in specific interactions with three residues on the EryK BC loop (Met 86, His 88, and Glu 89), which is one of the secondary structure elements involved in the EryK open-to-closed structural transition.[22] We proposed that the methyl group on 3′-OH, introduced during the conversion of mycarose to cladinose (Figure 1), would interfere with the closure of the enzyme on the substrate, due to the collision with Met 86, His 88, and Glu 89 on the BC loop, thus preventing a productive enzyme binding event and catalysis.

In this work, the three residues of the BC loop involved in direct interactions with the mycarosyl moiety have been mutated to allow ErB to accommodate the bulky methoxyl group of cladinose in the region of the active site that normally accepts the hydroxyl function of mycarose.

In more detail, Met 86 was substituted with an alanine (M86A) in order to provide space to the methyl group on the 3′-OH of cladinose. His 88 was mutated to glutamate (H88E) with the aim of reducing the steric hindrance of the side chain, by carrying out a polar amino acid to polar amino acid substitution. Finally, Glu 89 was substituted with a leucine

Table 2. Data Collection, Refinements, Statistics, and Validation for the M86A−ErB Structure[a]

Data Collection	
resolution (Å)	30.00−2.00 (2.03−2.00)
total measurements	278920
unique reflections	27774
completeness (%)	98.3 (77.4)
redundancy	3.9 (3.1)
R_{merge}[b] (%)	8.6 (44.4)
I/σ (I)	13.0 (2.1)
Wilson *B*-value (Å^2)	16.8
Refinement	
resolution (Å)	29.12−2.00 (2.03−2.00)
reflections	25901
molecules per asymmetric unit	1
space group	$P2_1$
unit cell (Å, deg)	a = 57.75,
	b = 36.60,
	c = 96.27,
	β = 92.93
R_{work}/R_{free}[c] (%)	16.3/21.5
Mean *B*-Factors (Å^2)	
protein	16.8
heme	8.5
substrate (ErB)	11.2
water/iron	26.7/9.8
Deviation from Ideal Geometry	
bond (Å)	0.015
angles (deg)	1.387
Ramachandran (%) favored/allowed/outliers	97.6/2.1/0.3
Number of Atoms	
protein	3540
heme/ligand	42/43
water	380
solvent content (%)	33.04

[a]The highest-resolution shell is shown in parentheses. [b]$R_{merge} = \Sigma_i\Sigma_j|I_{i,j} - \langle I_j\rangle|/\Sigma_i\Sigma_j I_{i,j}$, where i runs over multiple observations of the same intensity, and j runs over all crystallographically unique intensities. [c]$R_{cryst} = \Sigma||F_{obs}| - |F_{calc}||/|F_{obs}|$, where $|F_{obs}| > 0$. R_{free} is based on 5% of the data randomly selected and is not used in the refinement.

(E89L) to supply the methyl group with a hydrophobic environment, maintaining the isostericity with the side chain of the wild type residue.

Equilibrium Binding Analyses and Steady-State Kinetics of Erythromycin C-12 Hydroxylation on ErD. At first, we analyzed the effect of the mutations on the binding and catalytic properties of the enzyme against the physiological substrate ErD. Equilibrium binding experiments were performed by measuring the absorbance spectra of the mutants, at a constant concentration of 2 μM, varying ErD concentration. The observed titrations, reported in Figure 2A, were fitted to a hyperbolic function (eq 1). The calculated dissociation constants K_D are reported in Table 1. Upon binding to ErD, the M86A and H88E mutants display a simple hyperbolic behavior, yielding the characteristic *type I* shift of the Soret peak. Both variants show affinity for the substrate of the same order of magnitude with respect to the wild type enzyme (Table 1).[18,22] In the case of the E89L mutant, the ErD binding reaction follows a more complex mechanism that involves at least two processes, giving the typical *type I* and a *reverse type I* shift of the Soret peak.[31−33] The apparent K_D values were estimated using a single hyperbolic fit for each individual phase (Table 1).

All mutants were then tested for their enzymatic activity against ErD, comparing their behavior with the catalytic efficiency observed with $EryK_{WT}$. A typical *in vitro* assay for measuring P450 activity uses as electron-donor the ferredoxin/ferredoxin NADP+ reductase system. Initial velocities were determined by monitoring the rate of absorbance decay of NADPH at 340 nm over time, assuming a 1:1 stoichiometric relationship between NADPH consumption and substrate hydroxylation.[18] Steady state kinetic constants were determined (eq 2), and the values obtained are reported in Table 1. Plots of initial rates as a function of substrate concentration for $EryK_{WT}$ and for each mutant are given in Figure 3A.

Data analysis reveals that the mutation on Met 86 preserves the catalytic activity of the enzyme, giving k_{cat} and K_M values comparable to those of $EryK_{WT}$. On the contrary, mutation of Glu 89 dramatically reduces the catalytic efficiency of ErD hydroxylation, while mutation of His 88 appears to affect only V_{max} (Table 1), giving a K_M value similar to that of the wild type.

Equilibrium Binding Analyses and Steady-State Kinetics of Erythromycin C-12 Hydroxylation on ErB. Binding properties of $EryK_{WT}$ and mutants were, then, investigated using the metabolic intermediate ErB as a substrate. Equilibrium binding experiments were performed by measuring the absorbance spectra of the enzyme, at a constant concentration of 2 μM, varying ErB concentration. In Figure 2B, the observed titrations are reported for the EryK species investigated and fitted to eq 1. K_D values are summarized in Table 1.

As previously observed by Lambalot et al.,[18] $EryK_{WT}$ affinity for ErB is at least 20-fold lower than that for ErD. H88E and E89L mutants also show scarce affinity for the metabolite E89L binding curve following a similar complex trend observed for ErD binding. Only the M86A mutant form shows enhanced affinity for ErB (Table 1).

The EryK variants were then tested for their enzymatic activity against ErB, by using the P450 enzymatic assay reported above. Analysis of the kinetic traces obtained at different ErB

Table 1. Binding and Hydroxylation of ErD and ErB by EryK Wild Type and Mutants

	ErD binding and hydroxylase activity				ErB binding and hydroxylase activity			
	K_D (μM)	K_M (μM)	V_{max} (μM s^{-1})	k_{cat}/K_M (M^{-1} s^{-1})	K_D (μM)	K_M (μM)	V_{max} (μM s^{-1})	k_{cat}/K_M (M^{-1} s^{-1})
$EryK_{WT}$	3.0 ± 0.1[22]	20 ± 10	0.76 ± 0.10	(0.038 ± 0.024)·10^6	75 ± 10	n.d.[a]	n.d.[a]	n.d.[a]
M86A	18 ± 1	43 ± 8	0.53 ± 0.03	(0.012 ± 0.001)·10^6	14 ± 1	75 ± 45	0.9 ± 0.2	(0.012 ± 0.008)·10^6
H88E	8.1 ± 0.4	30 ± 10	0.15 ± 0.01	(0.005 ± 0.001)·10^6	120 ± 50	n.d.[a]	n.d.[a]	n.d.[a]
E89L	1.2 ± 0.2	82 ± 44	0.08 ± 0.02	(0.0010 ± 0.0005)·10^6	13 ± 10 21 ± 20	n.d.[a]	n.d.[a]	n.d.[a]
	65 ± 18							

[a]n.d. = not determined due to the undetectable activity observed toward this substrate.

dx.doi.org/10.1021/bi400223j | *Biochemistry* 2013, 52, 3678−3687

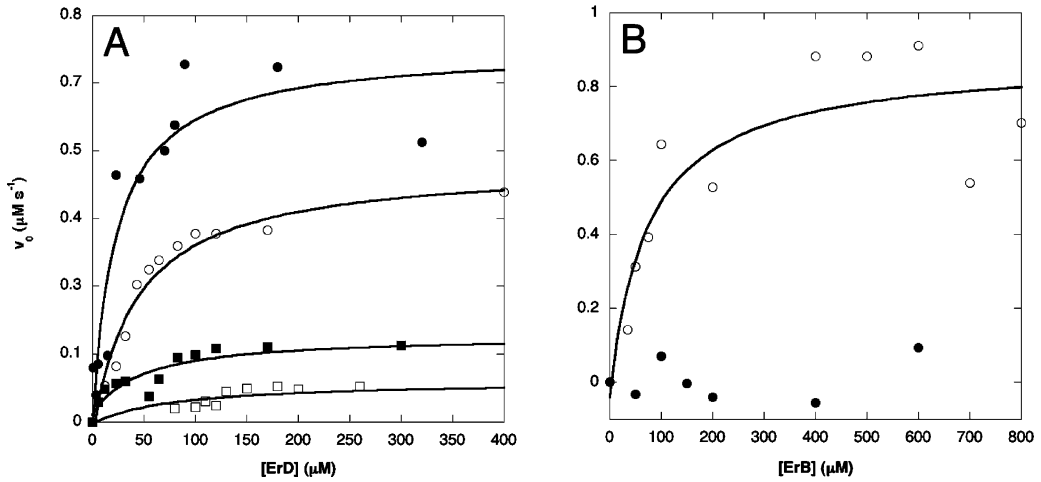

Figure 3. Initial rates of hydroxylation of $EryK_{WT}$ and mutants with ErD and ErB. Initial rates versus ErD (panel A) and ErB (panel B) concentrations are given for $EryK_{WT}$ (filled circles) and mutants (M86A, open circles; H88E, filled squares; and E89L, open squares). Initial rates were determined by applying a linear fit to the linear region of the time trace. Data were fitted to eq 2. In each experiment, absorbance was monitored at 340 nm by following the NADPH consumption over time at 303 K in 50 mM Tris·HCl at pH 7.5. Data on initial rates recorded for the $EryK_{WT}$-ErB reaction cannot be fitted to the Michaelis Menten equation, being essentially independent of ErB concentration. H88E and E89L kinetic data on ErB are not shown since there were no substrate concentration dependent activities, as observed for $EryK_{WT}$.

concentrations revealed $EryK_{WT}$ (Figure 3B) and the mutants H88E and E89L (data not shown) to be inactive against this substrate. However, we found the M86A mutant to display unequivocal hydroxylase activity on ErB (Figure 3B). The curve was fitted by using eq 2, and the calculated kinetic values are reported in Table 1.

GC/MS Analyses for Hydroxylation Product Determination. In order to examine the chemoselectivity of the reaction of hydroxylation catalyzed by M86A on ErB and to compare its behavior with the wild type enzyme, 70 μg of ErB was incubated separately with both $EryK_{WT}$ and M86A, along with the necessary cofactors and enzymes, and the distribution of products was analyzed by GC/MS, as described in Materials and Methods. Analysis of the chromatographic profile of the reaction mixture of ErB in the presence of M86A (Figure 4C) clearly shows the presence of a peak having the same retention time (13.39 min) and the same fragmentation pattern as those of authentic ErA (Figure S1, Supporting Information). The M86A mutant is able to convert approximately more than 40% of ErB into ErA after 1 h, without the formation of detectable side products. As expected, very low conversion of ErB to ErA (<5%, Figure 4B) was observed in the presence of the wild type enzyme, even after more than 1 h.

We have also evaluated the total efficiency of NADPH utilization for product formation. Indeed, as shown by other systems, although mutation M86A allows conversion of ErD to ErC, a reduced activity was observed since for $EryK_{WT}$ a 1:1.1 stoichiometry of NADPH:ErD consumption was observed, whereas for M86A a stoichiometry of 1:1.2 and 1:3.6 for NADPH:ErD and NADPH:ErB consumption, respectively, was observed (data not shown; see Materials and Methods for experimental details).

Crystallographic Structure Determination of the Mutant M86A in Complex with ErB. Experimental data on binding affinity and hydroxylation activity on ErB have shown that M86A EryK binds and converts ErB to ErA. In order to investigate the structural arrangement of M86A EryK in complex with ErB, we obtained, using a saturating concentration of the metabolite, crystals of the M86A−ErB complex (ErB−M86A), which diffracted to 2.0 Å resolution. Refinement of the ErB−M86A model yielded R_{cryst} = 16.3% and R_{free} = 21.5% (Table 2). The initial electron density omit map, calculated without including ErB in the model, revealed clear electron density in the active site that unambiguously corresponds to a molecule of ErB (Figure 5A).

The overall structure of ErB−M86A corresponds to the closed structure of the wild type enzyme in complex with the physiological substrate ErD (ErD−EryK, PDB code 2JJO[22]) (Figure S2, Supporting Information), the rmsd after superposition yields a value of 0.2 Å for C_α carbons. Inspection of the structure reveals that the presence of the mutation methionine to alanine in position 86 provides enough space to accommodate the methoxyl group on the C3′ of the cladinose moiety of ErB, allowing the rest of the molecule to arrange exactly as ErD in the active site of $EryK_{WT}$ (Figure 5), maintaining all the contacts that ensure its recognition. The rmsd on C_α carbons as a function of residue number has been reported in Figure S3 (Supporting Information). Neither the presence of the mutation nor the alternative substrate bound to the active site induces significant displacements with respect to the ErD−EryK structure even on the most flexible structural elements of EryK, BC loop (amino acids 65−95), FG loop (amino acids 175−182), the central part of helix I (amino acids 237−248), and β hairpin β_4 (amino acids 392−398), mainly responsible for substrate recognition and whose conformational changes are sensible to the nature of the ligand bound,[22,34] giving maximum displacement values not exceeding 1.0 Å (Figure S3, Supporting Information).

Figure 5A shows that the long side chain of methionine 86 has been replaced by a water molecule (Wat 228) that forms hydrogen bonds connecting His 88 on the BC loop with the C_α-carbonyl oxygen of Asn 233 on helix I and Wat 162, also absent in the wild type structure.[22] The position of cladinose is further constrained by direct hydrogen bonds with Glu 89 and with a bridging water molecule (Wat 84) between Glu 89 and Thr 83 on the BC loop and by van der Waals interactions with the FG loop that, in the case of the mycarosyl moiety of ErD, close on top of it (Figure 5B). Interestingly, His 88 assumes a

dx.doi.org/10.1021/bi400223j | Biochemistry 2013, 52, 3678−3687

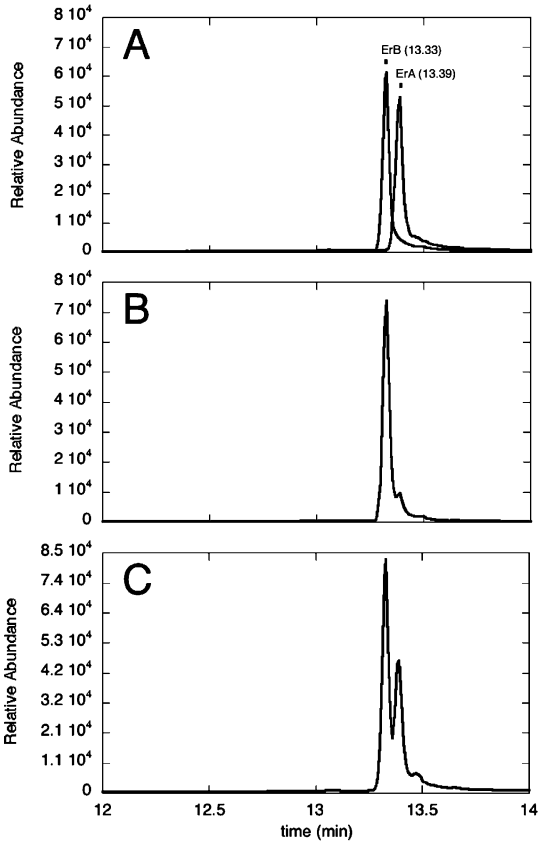

Figure 4. GC/SIM/MS chromatograms of hydroxylation products. (A) Gas-chromatographic profile of standard ErB (retention time: 13.33 min, European Pharmacopoeia Reference Standard) and standard ErA (retention time: 13.39 min, Sigma Aldrich, St.Louis, MO, USA). Retention times for both compounds are indicated on the top of the relative peak. (B) Chromatografic profile of the reaction mixture of ErB in the presence of $EryK_{WT}$ after 1 h. Less than 5% of ErB has been converted to ErA. (C) Chromatografic profile of the reaction mixture of ErB incubated with M86A enzyme after 1 h. A significant peak having the same retention time (and fragmentation profile; see Figure S1, Supporting Information) of ErA has been recorded, indicating that more than 40% of ErB has been converted to ErA.

double conformation (50% of occupancy for each rotamer) depending on the H-bond that its imidazole moiety establishes either with the methoxyl group of cladinose or with the above-mentioned Wat 228 (Figure 5A). The alternative conformations of His 88 do no affect the overall conformation of the BC loop. It represents the first structure of EryK in which this residue, essential for hydroxylase activity, displays enhanced flexibility.[22,34] All the other interactions of ErD in the active site observed in the wild type are conserved. On the C5 of the macrolactone ring of ErB, the desosamine moiety interacts with the loop at the C-terminal of helix K, establishing two H-bonds with Gln 290 (via Wat 46) and Gln 292 and the van der Waals contact with Ile 392 in the β-hairpin β4, previously found in the ErD−EryK structure (Figure 5A).

As in the wild type, C12 of the macrolactone ring, target of hydroxylation, is exposed to the heme-iron at a distance of 5.3 Å. A water molecule (Wat 63) has been found at 2.8 Å from the oxidized heme iron and is H-bonded to the hydroxyl group on the C11 of the substrate. Figure 5C shows that Wat 63 is involved in the water molecule chain (together with Wat 37 and Wat 34) that connects the active site to the bulk and that has been proposed to be responsible for proton delivery during the catalytic reaction.[22] Furthermore, as in the ErD−EryK structure, the hydrophobic contacts that the macrocycle establishes with the central residues of helix I (Ala 236, Leu 240, Ala 241, Ile 244, and Thr 245) lead to its overall bending and trigger a response of the whole structure that induces the closure of the active site (Figure 5B−C). Notably, in the presence of ErB in the active site, His 243 on helix I and Ser 166 on helix F, two of the key residues responsible for the conformational changes of EryK,[22] adopt a double conformation, mutually rotated of 180°, maintaining the H-bond interaction between the two side chains; such an interaction causes Trp 165 to interact with Pro 192 on helix G. The consequence of this network of interactions (previously called HSWP network,[22,34]) is the kink of the external helix G that drives the FG loop in hydrophobic contact with the BC loop, thus locking the closure of the active site (Figure 5B).

In conclusion, the substitution of M86A allows the accommodation of the extra methyl group of ErB, with local perturbation and compensation in the region of Ala 86. However, all of the fine interactions found in the ErD−EryK complex are preserved, and the closure and locking of the active site are reproduced in the ErB−M86A complex. The variation of kinetic parameters, leading to a 30% decrease of k_{cat}/K_M in the M86A mutant suggests weaker binding and a more open active site. Nevertheless, this is not evident upon comparing the ErD−$EryK_{WT}$ complex to the ErB−M86A complex, where thermal *B*-factors for the BC loop are comparable.

DISCUSSION

Unveiling fundamental structure−function relationships in P450s represents the basic tool to rationally manipulate these enzymes and tame their unique catalytic properties for defined applications.

In the present work, a structure-based rational design approach has been used on the bacterial P450 EryK to generate a substrate-specificity altered enzyme that, still maintaining enzymatic activity on its physiological substrate ErD, is able to react with the unnatural metabolite ErB and to convert it into the antibiotic product ErA. The achieved substrate promiscuity of the mutant could avoid the accumulation of ErB as shunt product in the ErA biosynthetic pathway, thus improving the yield and purity of the commercial product even during the fermentation stage.

Taking advantage of the three-dimensional structure of EryK in complex with the substrate ErD,[22] we identified three key residues involved in ErD recognition and responsible for the EryK discrimination against ErB. Met 86, His 88, and Glu 89 have been mutated with the specific aim to enhance binding and catalytic activity on ErB with respect to the wild type enzyme. Equilibrium binding experiments and enzymatic activity assays performed on three single site-directed mutants (M86A, H88E, and E89L) versus ErB revealed that the mutation on Met 86 to Ala met our purposes. This mutant form of EryK is able to convert more than 40% of ErB into ErA in 1 h, as confirmed by GC/MS analyses. Importantly, this mutation does not substantially compromise binding and activity of the enzyme to the physiological substrate ErD. Therefore, we may conclude that indeed the steric clash between Met 86 and the additional methoxyl group on cladinose is the factor preventing EryK from binding ErB. Moreover, analyzing the crystallographic structure of the ErB−M86A complex, we observed an unforeseen structural feature

dx.doi.org/10.1021/bi400223j | *Biochemistry* 2013, 52, 3678−3687

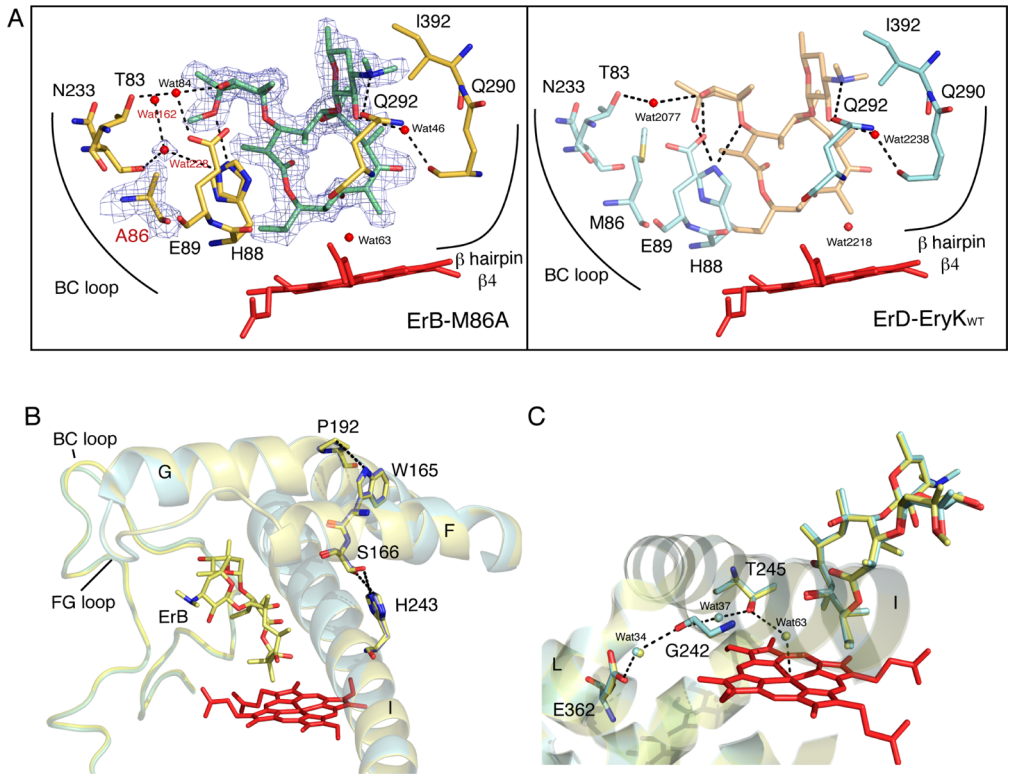

Figure 5. ErB in the active site of M86A enzyme: comparison with the ErD−EryK structure. (A) Sticks representation of the M86A amino acids that interact with the metabolite ErB, light green (ErB−M86A, light yellow, left panel), and of the $EryK_{WT}$ amino acid interacting with ErD, light orange (ErD−EryK, cyan sticks, right panel; PDB code 2JJO[22]). Electron density omit map ($2F_o - F_c$) is contoured at 1.0 σ around ErB, Ala 86, and Wat 288. Ala 86, Wat 162, and Wat 228 are labeled in red. B, BC loop, helices F, G, and I, and the organization of the residues involved in the HSWP network are shown for the ErB−M86A structure (light yellow) superposed on ErD−EryK (cyan sticks). (C) View of the proton shuttle pathway possibly involved in proton delivery during the catalytic reaction in ErB−M86A superposed on ErD−EryK (cyan sticks). Dashed lines indicate H-bonds and, in panel B, close contacts (within 4 Å). The heme group is in red sticks. Water molecules are labeled and represented as spheres. Superposition was based on secondary structure motifs as implemented in COOT.[30]

since the presence of Ala instead of Met 86 induces a reorganization of water molecules around the cladinose moiety, thus allowing network stabilizing interactions with ErB, favoring the closure and locking of the enzyme and the progress of the catalytic reaction.

Despite the fact that the H88E and E89L mutants have proved to be unsuccessful in ErB binding and conversion, binding and hydroxylase activity data on ErD confirmed their functional relevance given that both substitutions lead to mutant proteins with altered enzymatic properties. The E89L mutant displays, together with an unusual binding curve, an extremely reduced hydroxylase activity, thus pointing out the relevance of this residue for ErD recognition and conversion. However, the mutation on His 88 results in an enzyme that appears still able to bind ErD, but unsuitable to efficiently carry out the catalytic reaction, leading to a more than 7-fold reduction of turnover number. Further investigations are required to clarify the mechanisms underlying both the complex ErD binding process observed with E89L and the altered catalytic efficiency observed for H88E.

Several successful cases of P450 engineering have been reported, either upon rational design or by random mutagenesis and directed evolution approaches.[35−38] Nevertheless, a systematic use in industry of engineered P450s, such as the application in bioreactors for large-scale production of drugs, is still limited by enzyme instability in extreme conditions (pH, temperature, and organic solvent) and, more relevantly, by the necessity to couple a regulated process of feeding electrons for the complex catalytic cycle of P450s that can be achieved only enzymatically.[39] Our work proposes the rationally modified P450 EryK with altered specificity to be employed within the context of its original biosynthetic pathway allowing its use for the production of ErA with lower ErB contamination in a straightforward manner, by genetic modification of pre-existing strains. Further optimization of EryK by mutational studies might be required to increase the efficiency of the reaction. Even though its actual use requires other aspects of its industrial applicability to be addressed, it represents a promising alternative strategy in the effort to improve the production of ErA and its derivatives.

■ ASSOCIATED CONTENT

Supporting Information

EI mass spectrum of ErA from the reaction mixture containing ErB in the presence of M86A mutant; ribbon representation of the whole superposed structure of ErB-M86 and ErD-$EryK_{WT}$; and rmsd on C_α carbons, calculated superposing ErB-M86A and ErD-EryK structures, as a function of the residue number. This material is available free of charge via the Internet at http://pubs.acs.org.

Accession Codes

The atomic coordinates and the structure factors were deposited under the code 3ZKP in the Protein Data Bank

Research Collaboratory for Structural Bioinformatics, Rutgers University, New Brunswick, NJ (http://www.rcsb.org).

AUTHOR INFORMATION

Corresponding Author

*Tel: +39 06 49910548. Fax: +39 06 4440062. E-mail: beatrice.vallone@uniroma1.it (B.V.); linda.savino@uniroma1.it (C.S.).

Author Contributions

§B.V. and C.S. equally contributed to this work.

Funding

We are grateful to synchrotron ESRF (beamline ID23.2, Grenoble, France). The European Community-Research Infrastructure Action under FP7/2007-2013 under grant agreement number 226716 is acknowledged. This work was supported by grants from Italian MIUR FIRB2007 RBRN07BMCT.

Notes

The authors declare the following competing financial interest(s): L.C.M., B.V., and C.S. are listed as inventors on a patent application on "Cytochrome P450 Mutant for Optimizing Erythromycin A Production" (MI2012A001864).

ACKNOWLEDGMENTS

We thank Barrie Wilkinson, Rachel Lill (Biotica Technology, Ltd., UK), and Steven G. Kendrew for the kind gift of erythromycin D. The crystallographic experiments were performed on the ID23.2 beamline at the European Synchrotron Radiation Facility (ESRF), Grenoble, France. We are grateful to David Flot and Max Nanao at the ESRF for providing assistance in using beamline ID23.2. European Community-Research Infrastructure Action under Contract RII3-CT-2004-506008 from the FP6 "Structuring the European Research Area Programme". We thank M. Fornara for skillful support during experimental manipulations.

ABBREVIATIONS

P450, cytochrome P450; EryK, erythromycin D C12-hydroxylase; $EryK_{WT}$, erythromycin D C12-hydroxylase wild type; EryG, erythromycin *O*-methyltransferase; ErA, erythromycin A; ErD, erythromycin D; ErB, erythromycin B; ErC, erythromycin C; Ers, erythromycin intermediates; ^{10}ErD-EryK, EryK in complex with ErD; ErB-M86A, M86A mutant in complex with ErB; M86A, methionine 86 mutated to alanine; H88E, histidine 88 mutated to glutamate; E89L, glutamate mutated to leucine; DMSO, dimethyl sulfoxide; Tris, 2-amino-2-hydroxymethyl-propane-1,3-diol; NADPH, nicotinamide adenine dinucleotide phosphate reduced; $NADP^+$, nicotinamide adenine dinucleotide phosphate; GC/MS, gas chromatography−mass spectrometry analysis; SIM, selected ion monitoring; PDB, Protein Data Bank; EI, electron ionization; NIST, National Institute of Standard Technology

REFERENCES

(1) Griffith, R. S., and Black, H. R. (1970) Erythromycin. *Med. Clin. North Am. 54* (5), 1199−1215.

(2) Mahajan, G. B., and Balachandran, L. (2012) Antibacterial agents from actinomycetes - a review. *Front. Biosci. 1*, 240−253.

(3) Staunton, J., and Wilkinson, B. (1997) Biosynthesis of erythromycin and rapamycin. *Chem. Rev.*, 97.

(4) Washington, J. A., II, and Wilson, W. R. (1985) Erythromycin: a microbial and clinical perspective after 30 years of clinical use (2). *Mayo Clin. Proc. 60* (4), 271−278.

(5) Washington, J. A. N., and Wilson, W. R. (1985) Erythromycin: a microbial and clinical perspective after 30 years of clinical use (1). *Mayo Clin. Proc. 60* (3), 189−203.

(6) Kirst, H. A., and Sides, G. D. (1989) New directions for macrolide antibiotics: structural modifications and in vitro activity. *Antimicrob. Agents Chemother. 33* (9), 1413−1418.

(7) Asaka, T., Manaka, A., and Sugiyama, H. (2003) Recent developments in macrolide antimicrobial research. *Curr. Top. Med. Chem. 3* (9), 961−989.

(8) Djokić, S., Kobrehel, G., and Lazarevski, G. (1987) Erythromycin series. XII. Antibacterial in vitro evaluation of 10-dihydro-10-deoxo-11-azaerythromycin A: synthesis and structure-activity relationship of its acyl derivatives. *J. Antibiot 40* (7), 1006−1015.

(9) Ma, X., Zhanga, L., Wangb, R., Caoa, J., Liua, C., Fanga, Y., Wanga, J., and Ma, S. (2011) Novel C-4″ modified azithromycin analogs with remarkably enhanced activity against erythromycin-resistant *Streptococcus pneumoniae*: The synthesis and antimicrobial evaluation. *Eur. J. Med. Chem. 46* (10), 5196−5205.

(10) Morimoto, S., Takahashi, Y., Watanabe, Y., and Omura, S. (1984) Chemical modification of erythromycins. I. Synthesis and antibacterial activity of 6-O-methylerythromycins A. *J. Antibiot. 37* (2), 187−189.

(11) Saverino, D., Debbia, E. A., Pesce, A., Lepore, A. M., and Schito, G. C. (1992) Antibacterial profile of flurithromycin, a new macrolide. *J. Antimicrob. Chemother. 30* (3), 261−272.

(12) Yassin, H. M., and Dever, L. L. (2001) Telithromycin: a new ketolide antimicrobial for treatment of respiratory tract infections. *Expert Opin. Invest. Drugs 10* (2), 353−367.

(13) Woodward, R. B., and Logusch, E. (1981) Asymmetric total synthesis of erythromycin. *J. Am. Chem. Soc. 103* (11), 3210−3217.

(14) Adrio, J. L., and Demain, A. L. (2006) Genetic improvement of processes yielding microbial products. *FEMS Microbiol. Rev. 30* (2), 187−214.

(15) Kibwage, I. O., Hoogmartens, J., Roets, E., Vanderhaeghe, H., Verbist, L., Dubost, M., Pascal, C., Petitjean, P., and Levol, G. (1985) Antibacterial activities of erythromycins A, B, C, and D and some of their derivatives. *Antimicrob. Agents Chemother. 28*, 630−633.

(16) European Directorate for the Quality of Medicines and HealthCare (2011) *European Pharmacopoeia*, 7th ed., Supplement 7.3−7.5 Pack, European Directorate for the Quality of Medicines and HealthCare, Strasbourg, France.

(17) Stassi, D. L., Donadio, S., Staver, M. J., and Katz, L. (1993) Identification of a Saccharopolyspora erythraea gene required for the final hydroxylation step in erythromycin biosynthesis. *J. Bacteriol. 175*, 182−189.

(18) Lambalot, R. H., Cane, D. E., Aparicio, J. J., and Katz, L. (1995) Overproduction and characterization of the erythromycin C-12 hydroxylase, EryK. *Biochemistry 34*, 1858−1866.

(19) Chen, Y., Deng, W., Wu, J., Qian, J., Chu, J., Zhuang, Y., Zhang, S., and Liu, W. (2008) Genetic modulation of the overexpression of tailoring genes eryK and eryG leading to the improvement of erythromycin A purity and production in *Saccharopolyspora erythraea* fermentation. *Appl. Environ. Microbiol. 74*, 1820−1828.

(20) Zou, X., Zeng, W., Chen, C., Qi, X., Qian, J., Chu, J., Zhuang, Y., Zhang, S., and Li, W. (2010) Fermentation optimization and industrialization of recombinant *Saccharopolyspora erythraea* strains for improved erythromycin A production. *Biotechnol. Bioprocess Eng. 15*, 959−968.

(21) Wu, J., Zhang, Q., Deng, W., Qian, J., Zhang, S., and Liu, W. (2011) Toward improvement of erythromycin A production in an industrial *Saccharopolyspora erythraea* strain via facilitation of genetic manipulation with an artificial attB site fro specific recombination. *Appl. Environ. Microbiol. 77*, 7508−7516.

(22) Savino, C., Montemiglio, L. C., Sciara, G., Miele, A. E., Kendrew, S. G., Jemth, P., Gianni, S., and Vallone, B. (2009) Investigating the structural plasticity of a cytochrome P450: three-dimensional structures of P450 EryK and binding to its physiological substrate. *J. Biol. Chem. 284*, 29170−29179.

(23) Savino, C., Sciara, G., Miele, A. E., Kendrew, S. G., and Vallone, B. (2008) Cloning, expression, purification, crystallization and preliminary X-ray crystallographic analysis of C-12 hydroxylase EryK from *Saccharopolyspora erythraea*. *Protein Pept. Lett. 15*, 1138−1141.
(24) Tsuji, K., and Robertson, J. H. (1971) Determination of erythromycin and its derivatives by gas-liquid chromatography. *Anal. Chem. 43* (7), 818−821.
(25) Ducruix, A., and Giegè, R., Eds. (1992) Crystallization by Vapour Diffusion Methods, *Crystallization of Nucleic Acids and Proteins*, pp 82−89, Oxford University Press, Oxford, U.K.
(26) Minor, W., Tomchick, D., and Otwinoski, Z. (2000) Strategies for macromolecular synchrotron crystallography. *Structure 8*, R105−110.
(27) Collaborative Computational Project, N (1994) The CCP4 suite: programs for protein crystallography. *Acta Crystallogr., Sect. D 50*, 7690−7763.
(28) Pannu, N. J., Murshudov, G. N., Dodson, E. J., and Read, R. J. (1998) Incorporation of prior phase information strengthens maximum-likelihood structure refinement. *Acta Crystallogr., Sect. D 54*, 1285−1294.
(29) Emsley, P., Lohkamp, B., Scott, W. G., and Cowtan, K. (2010) Features and development of Coot. *Acta Crystallogr., Sect. D 66*, 486−501.
(30) Emsley, P., and Cowtan, K. (2004) Coot: model-building tools for molecular graphics. *Acta Crystallogr., Sect. D 60*, 2126−2132.
(31) Kumaki, K., Sato, M., Kon, H., and Nebert, D. W. (1978) Correlation of type I, Type II, and reverse type I difference spectra with absolute changes in spin state of hepatic microsomal cytochrome P-450 iron from five mammalian species. *J. Biol. Chem. 253*, 1048−1058.
(32) Ouellet, H., Kells, P. M., Ortiz de Montellano, P. R., and Podust, L. M. (2011) Reverse type I inhibitor of *Mycobacterium tuberculosis* CYP125A1. *Bioorg. Med. Chem. Lett. 21* (1), 332−337.
(33) Raag, R., and Poulos, T. L. (1989) The structural basis for substrate-induced changes in redox potential and spin equilibrium in cytochrome P-450cam. *Biochemistry 28*, 917−922.
(34) Montemiglio, L. C., Gianni, S., Vallone, B., and Savino, C. (2010) Azole drugs trap cytochrome P450 EryK in alternative conformational states. *Biochemistry 49*, 9199−9206.
(35) Farinas, E. T., Bulter, T., and Arnold, F. H. (2001) Directed enzyme evolution. *Curr. Opin. Biotechnol. 12*, 545−551.
(36) Jung, S. T., Lauchli, R., and Arnold, F. H. (2011) Cytochrome P450: taming a wild type enzyme. *Curr. Opin. Biotechnol. 22*, 1−9.
(37) Rabe, K. S., Gandubert, V. J., Spengler, M., and Niemeyer, C. M. (2008) Engineering and assaying of cytochrome P450 biocatalysts. *Anal. Bioanal. Chem. 392*, 1059−1073.
(38) Whitehouse, C. J., Bell, S. G., and Wong, L. L. (2012) P450(BM3) (CYP102A1): connecting the dots. *Chem. Soc. Rev. 41* (3), 1218−1260.
(39) Gillam, E. M. J. (2008) Engineering cytochrome P450 enzymes. *Chem. Res. Toxicol. 21* (1), 220−231.